European Journal of Human Genetics (2014) 22, 497–504

www.nature.com/ejhg

ARTICLE

New *TRPM6* missense mutations linked to hypomagnesemia with secondary hypocalcemia

Sergio Lainez[1,2,6], Karl Peter Schlingmann[3,6], Jenny van der Wijst[4], Bernd Dworniczak[5], Femke van Zeeland[1], Martin Konrad[3], René J Bindels[1] and Joost G Hoenderop*[,1]

Despite recent progress in our understanding of renal magnesium (Mg^{2+}) handling, the molecular mechanisms accounting for transepithelial Mg^{2+} transport are still poorly understood. Mutations in the *TRPM6* gene, encoding the epithelial Mg^{2+} channel TRPM6 (transient receptor potential melastatin 6), have been proven to be the molecular cause of hypomagnesemia with secondary hypocalcemia (HSH; OMIM 602014). HSH manifests in the newborn period being characterized by very low serum Mg^{2+} levels (<0.4 mmol/l) accompanied by low serum calcium (Ca^{2+}) concentrations. A proportion of previously described *TRPM6* mutations lead to a truncated TRPM6 protein resulting in a complete loss-of-function of the ion channel. In addition, five-point mutations have been previously described. The aim of this study was to complement the current clinical picture by adding the molecular data from five new missense mutations found in five patients with HSH. To this end, patch-clamp analysis and cell surface measurements were performed to assess the effect of the various mutations on TRPM6 channel function. All mutant channels, expressed in HEK293 cells, showed loss-of-function, whereas no severe trafficking impairment to the plasma membrane surface was observed. We conclude that the new *TRPM6* missense mutations lead to dysregulated intestinal/renal Mg^{2+} (re)absorption as a consequence of loss of TRPM6 channel function.
European Journal of Human Genetics (2014) **22,** 497–504; doi:10.1038/ejhg.2013.178; published online 14 August 2013

Keywords: TRPM6; distal convoluted tubule; HSH; hypomagnesemia

INTRODUCTION

Hypomagnesemia with secondary hypocalcemia (HSH) is a rare autosomal-recessive disease that appears in early infancy and is characterized by generalized convulsions preceded sometimes by other signs of increased neuromuscular excitability like muscle cramps and agitation.[1] Impaired synthesis and secretion of parathyroid hormone (PTH) as a consequence of profound hypomagnesemia have been suggested to be responsible for the observed hypocalcemia.[2,3] Early diagnosis is decisive to avoid neurological problems that can lead to permanent neurological injury or even sudden death as a consequence of arrhythmias in extreme cases.[4,5] In HSH patients, serum magnesium (Mg^{2+}) levels dramatically fall below the normal range (0.2–0.4 *vs* 0.70–0.95 mmol/l).[6,7]

The body's Mg^{2+} balance is tightly regulated by a concerted action of intestinal absorption and excretion/reabsorption of Mg^{2+} via the kidney. The majority of renal-filtered Mg^{2+} is reabsorbed in the proximal tubule and the thick ascending limb of the loop of Henle via a passive paracellular transport process.[8] Subsequently, fine-tuning of Mg^{2+} excretion takes place in the distal convoluted tubule (DCT), where Mg^{2+} is reabsorbed via an active transcellular pathway.[9] Extensive genetic analyses of different families suffering from HSH led to the identification of the *TRPM6* gene as an essential player for systemic Mg^{2+} regulation, as emphasized by the severe drop in serum Mg^{2+} levels together with renal Mg^{2+} wasting in those patients.[10,11] TRPM6 functions as a constitutively active cation channel highly permeable to Mg^{2+}. Intracellular Mg^{2+} levels regulate its activity by means of a feedback inhibition mechanism.[12] TRPM6 has a restricted expression pattern along the apical membranes of small intestine and DCT.[13] These characteristics, together with the identification of mutations in *TRPM6* linked to HSH,[10,11] highlight its important role in epithelial Mg^{2+} handling.

Earlier reported *TRPM6* mutations mainly lead to stop, frame-shift and splice-site mutations as well as deletion of exons, thereby greatly affecting the key structural features of the TRPM6 protein.[10,11,14–17] So far, there are two missense mutations described previously, $S^{141}L$ and $P^{1017}R$, resulting in either trafficking or gating impairment of TRPM6.[18,19] Another three-point mutations leading to HSH, where the underlying molecular mechanism was not disclosed, have also been published.[20]

Here, we characterize a new set of five missense mutations identified in five HSH patients. The functional consequence of these novel mutations was studied in mammalian Human embryonic kidney (HEK) 293 cells by electrophysiological and biochemical analyses.

MATERIAL AND METHODS

Patients and families

The study cohort comprises five families from different ethnic origin with seven individuals with HSH and at least one missense mutation leading to a non-conservative amino-acid exchange in TRPM6 (Table 1). These five

[1]Department of Physiology, Radboud University Nijmegen Medical Centre, Nijmegen Centre for Molecular Life Sciences, Nijmegen, The Netherlands; [2]Department of Pharmacology, University of Cambridge, Cambridge, UK; [3]Department of General Pediatrics, University Hospital Münster, Münster, Germany; [4]MRC Protein Phosphorylation Unit, College of Life Sciences, University of Dundee, Dundee, Scotland, UK; [5]Department of Human Genetics, Westfaelische Wilhelms Universität, Münster, Germany
[6]These authors contributed equally to this work.
*Correspondence: Professor JG Hoenderop, Department of Physiology, Radboud University Nijmegen Medical Centre, Nijmegen Centre for Molecular Life Sciences, P.O. Box 9101, Nijmegen 6500 HB, The Netherlands. Tel: +31 24 3610580; Fax: +31 24 3616413; E-mail: J.Hoenderop@fysiol.umcn.nl
Received 13 December 2012; revised 20 June 2013; accepted 11 July 2013; published online 14 August 2013

Table 1 Clinical and biochemical data of genetically characterized HSH patients

Patient	*F35.1*	*F37.1*	*F38.1*	*F40.1*	*F46.1*	*Means from previous cohort* [16]
Gender	M	F	F	F	F	
Origin	East Indian	Turkish	Turkish	North American	European	
Parental consanguinity	No	Yes	No	No	No	
Age at manifestation	2 months	Infancy	4 months	6 weeks	9 months	2 months
Age of diagnosis	5 months	Infancy	8 months	6 weeks	4 years	2 months
Initial symptoms	Seizure	Seizure	Seizure	Seizure	Seizure	
Initial S-Mg (mM)	0.08	0.05	0.20	0.12	0.10	0.20
Initial S-Ca (mM)	1.94	1.78	1.60	1.60	1.47	1.65
Initial therapy	Mg2+ iv	Mg2+ iv	Mg2+ iv	Ca2+ and Mg2+ iv	Mg2+ im and po	
Follow-up (years)	6	19	1.8	0.4	3	
Maintenance Mg-therapy (mmol/kg/day)	0.75	0.97	0.50	1.86	1.50	0.93
S-Mg (mM)*	0.69	0.50	0.53	0.82	0.67	0.55
Total S-Ca (mM)*	2.42	2.40	2.3	?	2.67	2.40
Nucleotide change	[c.3428T>C]+ [c.2391+2T>G]	c.3158A>G	[c.469G>T]+ [c.5261G>A]	[c.5084-2A>G]+ [c.2123T>C]	[c.2615A>G]+ [c.4988A>G]	
Zygosity	comp.-het	homoz	comp.-het	comp.-het	comp.-het	
Consequence on protein level	p.L1143P+ splice site loss	p.Y1053C	p.E157X+ p.S1754N	p.L708P+ Splice site loss	p.E872G+ p.Q1663R#	

Abbreviations: iv, intravenously; im, intramuscularly; po, per os; *, under substitution; ?, unknown value; #, SNP rs55679040.

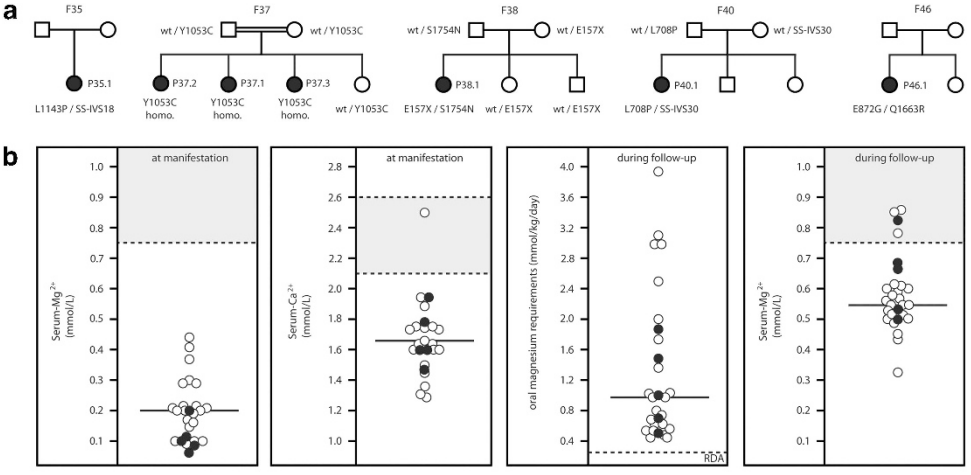

Figure 1 Family pedigrees and clinical data of patients with HSH. Panel **a** shows the five family pedigrees. Affected family members are indicated by black circles (girls) and squares (boys). The double horizontal line in the diagram for family 37 indicates parental consanguinity. Mutation analysis is shown for patients as well as for parents in families F37, F38 and F40. Panel **b** shows levels of serum Mg^{2+} and Ca^{2+} at manifestation, the dosage of oral Mg^{2+} supplements during maintenance therapy as well as the serum Mg^{2+} levels measured during follow-up. The black circles indicate the values measured in the five index patients of this study. White circles indicated individual values obtained in a previously published cohort of patients with truncating TRPM6 mutations (Schlingmann *et al*[14]) to allow for a better comparison of phenotypes. The reference ranges for serum magnesium and calcium are indicated by gray shading, the recommended daily allowance for oral Mg^{2+} intake (0.25 mmol/kg/day) is indicated by a dashed line.

families are part of a larger cohort of a total of 53 families with genetically proven HSH (unpublished data). Parental consanguinity was noted in family F37. Family pedigrees are displayed in Figure 1. Clinical aspects of patient F46.1 were reported previously.[21] In all the affected patients, the diagnosis was based on manifestation in early childhood with severe hypomagnesemia accompanied by hypocalcemia, and relief of the observed clinical symptoms and normocalcemia upon administration of Mg^{2+} salts. Serum biochemical parameters were analyzed using the standard techniques. The ultrafiltrable fraction of serum Mg^{2+} was calculated as $UF_{Mg} = 0.7 \times S_{Mg}$.[22] Renal Mg^{2+} handling was assessed by calculating fractional Mg^{2+} excretions with $Fe_{Mg} = (U_{Mg} \times S_{Cr})/(UF_{Mg} \times U_{Cr} \times 100)$ where Fe is fractional excretion, S_{Mg} is serum Mg^{2+}, U_{Mg} is urinary Mg^{2+}, S_{Cr} is serum creatinine and U_{Cr} is urine creatinine. Renal ultrasound was performed to rule out nephrocalcinosis. The clinical course was evaluated retrospectively with a standardized questionnaire. Diarrhea as the main side effect of high oral Mg^{2+} administration was considered as three or more loose or watery bowel movements per day.

Mutation analysis

Isolation of DNA from blood was made using the standard procedures. Informed consent was obtained from the affected individuals and participating

relatives. Experimental procedures were in accordance with the standards of the medical ethics committee of each participating institution. For *TRPM6* mutational screening, an overlapping set of PCR primers based on the sequence of the human *TRPM6* gene (genomic contig GenBank accession no. AL354795) was used as a template to amplify the whole coding sequence (exons 1–39) as well as the intron/exon boundaries from genomic DNA (primer sequences available upon request). Amplified products were sequenced directly from both the strands.

DNA constructs

In brief, human *TRPM6* cDNA was subcloned into pCINeo/IRES-GFP vector using PCR.[23] Wild-type (WT) TRPM6 in the pCINeo/IRES-GFP vector was HA-tagged at the N-terminal tail as described previously.[13] Template pCINeo/IRES-GFP without TRPM6 was used as mock. TRPM6 mutants, depicted as $L^{708}P$, $E^{872}G$, $Y^{1053}C$, $L^{1143}P$ and $S^{1754}N$, as well as SNP rs55679040 ($Q^{1663}R$) were created using the QuikChange site-directed mutagenesis kit (Stratagene, La Jolla, CA, USA) according to the manufacturer's protocol. All constructs were verified by sequence analysis.

Electrophysiology and solutions

HEK293 cells were seeded as previously described.[24] Cells were transiently transfected with 1 μg of the respective constructs using Lipofectamine 2000 (Invitrogen-Life Technologies, Breda, the Netherlands). For co-transfection studies, 0.5 μg of both WT and respective mutants were used. The whole-cell configuration of the patch-clamp technique was used. To study TRPM6-evoked outward Na^+ currents, we applied a stimulation protocol consisting of repetitive voltage ramps from -100 to $+100$ mV over 450 ms duration every 2 s from a V_h of 0 mV. Current densities were obtained by normalizing the current amplitude to the cell membrane capacitance. The extracellular bath solution consisted of (in mmol/l): 150 NaCl, 1 $CaCl_2$, and 10 HEPES (pH 7.35 adjusted with NaOH). The intracellular solution consisted of (in mmol/l): 150 NaCl, 10 Na_2EDTA, and 10 HEPES (pH 7.2 adjusted with NaOH). The analysis and display of patch-clamp data were performed using Igor Pro software version 6.0 (WaveMetrics, Lake Oswego, OR, USA).

Biotinylation and immunoblotting

HEK293 cells were seeded on poly-L-lysine-coated six-well plates (1.1 million cells/well). After 4 h, cells were transiently transfected with either 1 μg ($Y^{1053}C$, $Q^{1663}R$, $S^{1754}N$ and WT) together with 1 μg of mock vector or 2 μg ($L^{708}P$, $E^{872}G$ and $L^{1143}P$) to obtain equal amount of input protein for all mutants and thereby compare membrane expression levels. After 48 h, cells were serum-starved overnight. Subsequently, proteins present at the cell surface were biotinylated with 0.5 mg/ml sulfo-NHS-LC-LC-Biotin (Pierce, Rockford, IL, USA) in PBS-CM for 30 min at 4 °C as previously described.[25] Immunoblots were incubated with mouse anti-HA (Cell Signalling Technology, Danvers, MA, USA). Blots were incubated with sheep horseradish peroxidase-conjugated anti-mouse (Jackson ImmunoResearch, West Grove, PA, USA) and then visualized using the enhanced chemiluminescence system.

Statistics

Data are presented as the mean ± standard error of the mean (SEM), with *n* representing the number of cells tested. Statistical analysis was performed with one-way ANOVA followed by Bonferroni *post-hoc* method using GraphPad Prism 4.0 (GraphPad, San Diego, CA, USA).

RESULTS

Clinical data/follow-up

Clinical symptoms and laboratory data recorded at initial manifestation and during follow-up are summarized in Table 1. The follow-up time of patients ranged from 0.4 to 19 years. In patients F38.1 and F40.1, hereditary Mg^{2+} deficiency was diagnosed at first manifestation, and maintenance Mg^{2+} therapy was prompted. In contrast, serum Mg^{2+} levels were not measured or hypomagnesemia was not noticed initially in patients F35.1, F37.1, and F46.1, which resulted in recurrent episodes of cerebral convulsions in patient F37.1. Patient F46.1 experienced two episodes of cerebral convulsions during infancy, each associated with a febrile illness and apparently remained asymptomatic until the age of 4 years when she was hospitalized with neurological symptoms. The delay of diagnosis as well as the repeated episodes of hypomagnesemia with consecutive cerebral convulsions due to malcompliance resulted in mental retardation in patient F37.1, whereas the other four patients showed a normal neurodevelopmental outcome. Unfortunately, only limited clinical data was available for patients F35.1 and F37.1, as well as for the two affected sisters of patient F37.1 (F37.2 and F37.3).

Serum Mg^{2+} levels at initial presentation ranged from 0.05 to 0.20 mmol/l; initial serum Ca^{2+} levels were 1.47–1.78 mmol/l. Figure 1 shows the individual values of patients reported here (black circles) in comparison to the values observed in a previously reported cohort of patients with truncating mutations (white circles).[14] PTH levels were only measured in patients F38.1 and F46.1 before initiation of treatment and were found to be low normal and low, respectively. After initiation of Mg^{2+} administration, serum Ca^{2+} levels rapidly returned to normal values and remained stable under Mg^{2+} maintenance therapy. PTH levels during follow-up, as far as available, were normal. Serum Mg^{2+} levels mainly failed to reach normal values under oral substitution and remained in the subnormal range (median 0.67 mmol/l); only patient F40.1 displayed normomagnesemia (Figure 1). Maintenance therapy generally consisted of an oral supplementation with different Mg^{2+} salts. Daily oral Mg^{2+} doses ranged from 0.50 to 1.86 mmol/kg per day, with a median of 0.97 mmol/kg per day (Figure 1).

Mutation analysis

Mutation analysis of the *TRPM6* gene revealed nine different mutations present in our cohort of five families (Table 1). In all the families, at least one mutant allele comprises a missense mutation leading to a non-conservative amino-acid exchange. In total, five missense mutations were identified. Whereas patient F37.1 is homozygous for mutation $Y^{1053}C$ (both parents being heterozygous and bearing the $Y^{1053}C$ missense mutation), patients F35.1, F38.1, and F40.1 display truncating mutations on the second allele (stop and splice-site mutations). In patient F46.1, only one missense mutation, $E^{872}G$, in heterozygous state could be identified. An additional sequence variant, $Q^{1663}R$, was detected which was unknown at time of discovery and therefore was initially suspected to represent a second pathogenic allele. As DNA of the parents was not available from the patients' parents, a segregation analysis was impossible. The $Q^{1663}R$ variant was later listed as a single-nucleotide polymorphism (SNP rs55679040) in public databases and appears in the exome variant server (http://www.evs.gs.washington.edu/EVS) with a frequency of 90 of 8590 alleles (allele frequency of $\sim$1.0%) in the European population.

Genotypes from parents of F35 patient could not be determined, whereas parents of F38.1 were both heterozygous: one bearing the $S^{1754}N$ mutation, and the another one having the $E^{157}X$ premature stop mutation. Parents from the F40.1 patient were also heterozygous, one of them carrying the mutation $L^{708}P$ and the other one having a splice-site mutation.

Except for mutation $E^{157}X$ identified in patient F38.1 that was described before in another Turkish family,[14] all other mutations are novel. Table 1 depicts the observed TRPM6 nucleotide exchanges and consequences for the TRPM6 amino-acid sequence/structure; Figure 4 shows a topological illustration of the TRPM6 protein with missense mutations indicated.

Functional characterization of TRPM6 mutants

To determine the functional implications of mutations on TRPM6 channel activity, HEK293 cells were transiently transfected with either mock, WT TRPM6, or the different TRPM6 mutants ($L^{708}P$, $E^{872}G$, $Y^{1053}C$, $L^{1143}P$, $S^{1754}N$, as well as variant $Q^{1663}R$). Mock-expressing cells showed low background endogenous currents (≈ 30 pA/pF), corresponding to TRPM7-like MagNum currents.[26,27] Averaged current density for WT was 195 ± 39 pA/pF, in line with previous studies in HEK293 cells, while a dramatic decrease in current amplitudes was observed for the $L^{708}P$, $E^{872}G$, $Y^{1053}C$, $L^{1143}P$, and $S^{1754}N$ mutants. Specifically, $L^{708}P$, $E^{872}G$, $L^{1143}P$, and $Y^{1053}C$ mutants showed outward currents comparable to the mock response (32 ± 5 pA/pF). The $S^{1754}N$ mutant evoked a residual current density (57 ± 10 pA/pF) that doubled the observed current in mock-expressing cells (Figure 2). In contrast, the $Q^{1663}R$ variant (SNP rs55679040) displayed current amplitudes comparable to WT (Figure 2).

$Q^{1663}R$ biophysical properties do not differ from those of WT TRPM6

To investigate whether the $Q^{1663}R$ sequence variant showed different functional behaviour with respect to WT TRPM6, we examined divalent-mediated block as previously shown by Li *et al*[28] and the response to epidermal growth factor (EGF) application.

Generation of a dose–response curve for divalent cation-mediated block did not give a different inhibitory value (IC_{50}). Specifically, IC_{50} for Mg^{2+} at -40 mV was 1.31 ± 0.02 μM compared to 1.27 ± 0.02 µM for TRPM6 and $Q^{1663}R$, respectively. Lower but not significantly different values for Ca^{2+} were recorded: 0.26 ± 0.03 and 0.23 ± 0.02 μM, respectively (data not shown). Next, we analyzed the EGF-mediated upregulation of TRPM6 outward currents as previously published by Groenestege *et al*.[29] Treatment of TRPM6-expressing HEK293 cells with 10 nM EGF for 30 min at 37 °C produced a 1.5-fold increase in WT TRPM6 compared to 1.33-fold for $Q^{1663}R$, which was not significantly different.

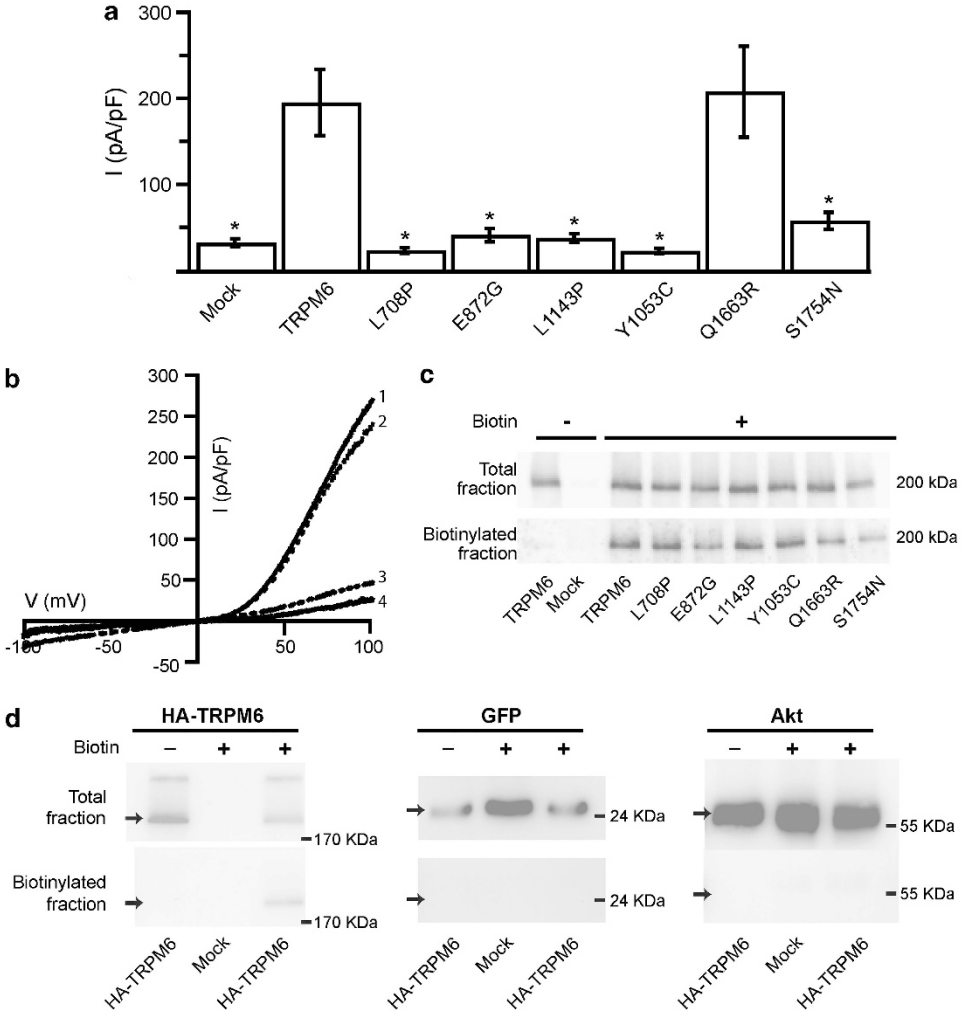

Figure 2 Functional analysis of WT and mutant TRPM6 channels transiently expressed in HEK293 cells. (**a**) Averaged current density at +80 mV after 200 s of mock, WT TRPM6, and mutant TRPM6 (≥ 10 cells per condition; $n = 3$ experiments). *$P < 0.05$ compared with WT. (**b**) Current–voltage (I/V) relationship from representative traces of WT TRPM6 (1), $Q^{1663}R$ SNP (2), $E^{872}G$ or $S^{1754}N$ mutants (3), and mock or the other mutants (4). (**c**) Cell surface biotinylation of mock, WT TRPM6, and mutant/SNP TRPM6 expressing HEK293 cells. TRPM6 expression was analyzed by immunoblotting for plasma membrane fraction (lower panel) and input from the total cell lysates (upper panel). Representative immunoblot of three independent experiments is shown. (**d**) Cell surface biotinylation of cytosolic proteins in HEK293 cells. Left panel shows TRPM6 expression and membrane-binding control, whereas the middle and left panels show no biotin bound to cytosolic proteins (GFP and Akt in this case). This control confirms that only membrane proteins are detected in our biotinylation assays.

Expression of TRPM6 mutants at the plasma membrane

Functional studies showed a dramatic decrease in outward currents of all mutants but not for SNP rs55679040 ($Q^{1663}R$ variant). To determine whether the loss of channel function was a consequence of impaired trafficking to the plasma membrane, we performed cell surface biotinylation studies in HEK293 cells expressing either WT TRPM6 or the TRPM6 mutants. Figure 2 reveals that WT TRPM6 and the mutants were expressed at the plasma membrane. Notably, WT and mutant TRPM6 channels were equally expressed in all the tested conditions, as determined in the total cell lysates (Figure 2, panel c). Labelling of plasma membrane TRPM6 by biotin was specific as cytoplasmic proteins were not biotinylated (Figure 2, panel d). These results argue against a trafficking problem that consequently could explain a reduction in current amplitude and thereby favor the hypothesis of a modification in TRPM6-gating properties.

Co-expression studies of $E^{872}G$ and $Q^{1663}R$

As the $E^{872}G$ mutation and the $Q^{1663}R$ variant (SNP rs55679040) occur together in patient F46.1, and our functional analysis suggested that the $Q^{1663}R$ variant functions almost equally as does WT TRPM6, we studied the combined effect of both sequence variants on TRPM6 channel function. Therefore, we performed cotransfections of TRPM6/TRPM6, TRPM6/$E^{872}G$, and $Q^{1663}R/E^{872}G$. Figure 3 shows that expression of the $E^{872}G$ mutant together with either WT TRPM6 or the $Q^{1663}R$ variant leads to a significant decrease in current amplitude. Importantly, coexpression of TRPM6 with the $E^{872}G$ mutant did not affect the amount of channels at the cell surface, whereas a ~10% decrease was observed when both variants were expressed together. Taken together, these results suggest a dosage-dependent effect of the $E^{872}G$ mutant on TRPM6 channel function rather than a dominant-negative effect.

DISCUSSION

The present work aimed to evaluate five non-related patients suffering from acute hypomagnesemia in early infancy. Their predominant symptom at initial presentation consisted of generalized seizures. Laboratory examination revealed the characteristic combination of profound hypomagnesemia (serum levels of 0.05–0.20 mmol/l), hypoparathyroidism, and consecutive hypocalcemia. Clinical and laboratory findings together pointed to the diagnosis of HSH as responsible for impairment in Mg^{2+} handling. The differential diagnosis can be complicated in these patients due to the very low serum Mg^{2+} levels as depicted in Table 1. The pathophysiology of HSH comprises a primary defect in intestinal Mg^{2+} uptake and an additional renal Mg^{2+} wasting.[10] The diagnosis of this hereditary disorder is sometimes delayed by the fact that renal Mg^{2+} wasting is not detectable during phases of profound hypomagnesemia.[30] As such, a low FE can be secondary to a renoprotective response in order to keep a normal plasmatic level concentration of Mg^{2+} or, as in this case, secondary to a massive depletion of the aforementioned ion in plasma. The gold test to differentiate between these two possibilities is to analyze the renal response or leaking after a load of Mg^{2+} to the patient in order to return to plasmatic homeostatic values (the so-called Mg^{2+} loading test). A renoprotective response after

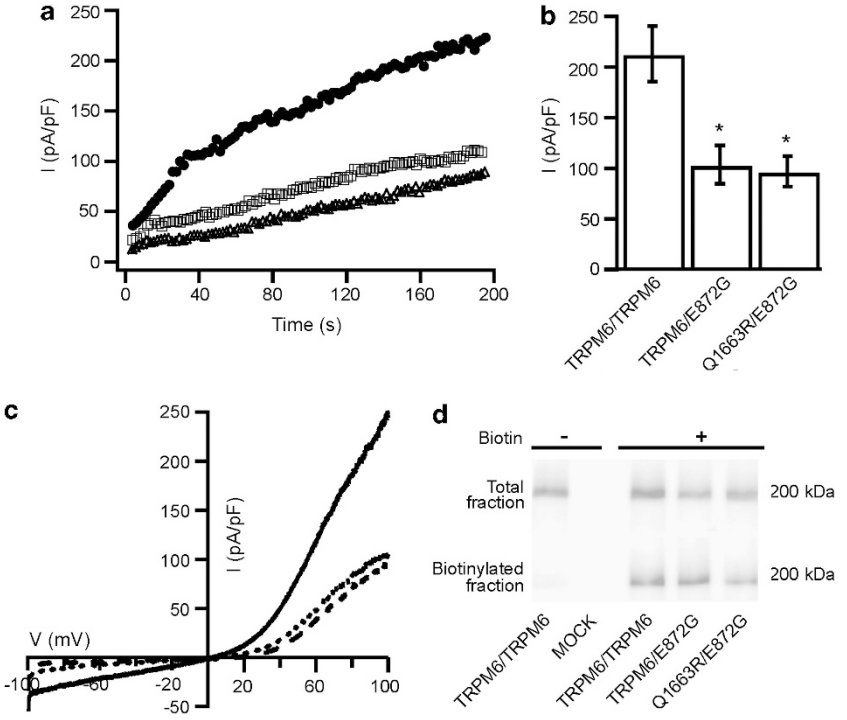

Figure 3 Functional effect of the $E^{872}G$ mutation. (**a**) Representative traces of the time course of the current density at +80 mV of TRPM6/TRPM6 (solid circles), TRPM6/$E^{872}G$ (open squares), and $Q^{1663}R/E^{872}G$ SNP and mutant (open triangles), $n \geq 15$ cells per condition; $n = 3$ experiments. (**b**) Averaged current density at +80 mV after 200 s of the indicated conditions. $^*P < 0.05$ compared with WT. (**c**) Current–voltage relationship from representative traces of TRPM6/TRPM6 (solid line), TRPM6/$E^{872}G$ (dotted line), and $Q^{1663}R/E^{872}G$ SNP and mutant (dashed line), $n \geq 15$ cells per condition; $n = 3$ experiments. (**d**) Cell surface biotinylation of mock, TRPM6/TRPM6, TRPM6/$E^{872}G$, and $Q^{1663}R/E^{872}G$ coexpressing HEK293 cells. TRPM6 expression was analyzed by immunoblotting for plasma membrane fraction (lower panel) and input from the total cell lysates (upper panel). Representative immunoblot of three independent experiments is shown.

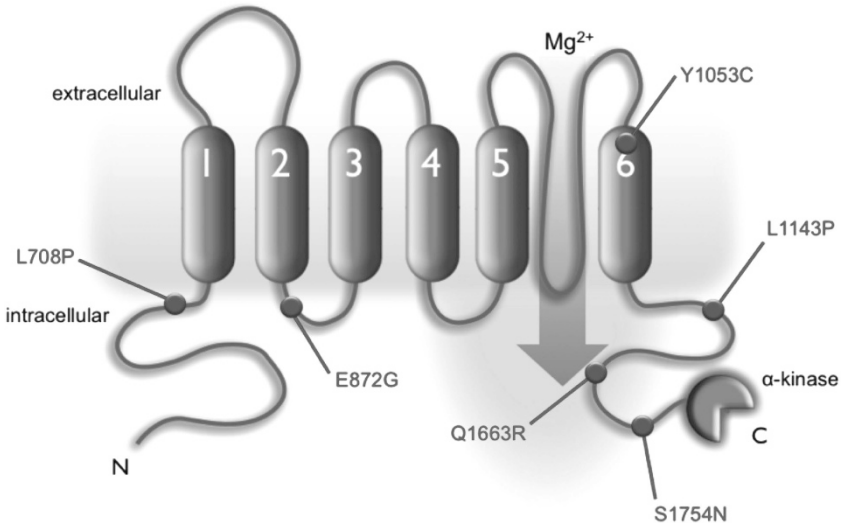

Figure 4 Topological illustration of a monomeric subunit of TRPM6. TRPM6 is exhibiting six putative transmembrane segments as well as intracellular N-terminal and C-terminal domains. It also contains its characteristic α-kinase domain at the C-terminus. The missense mutations and SNP found in the HSH patients are indicated in red. The full colour version of this figure is available at *European Journal of Human Genetics* online.

normalization of plasmatic levels will automatically exclude HSH, whereas a renal leaking that becomes apparent after Mg^{2+} infusion will support the diagnosis.

Several mutations in TRPM6 have been associated with HSH in patients. The majority of them are predicted to cause a premature termination of TRPM6. These include stop mutations, splice-site mutations, frame-shift mutations, and deletions.[10,14–17,20,31] Furthermore, five missense mutations leading to HSH have been described so far, from which only $S^{141}L$ and $P^{1017}R$ were further studied at the molecular level.[10,19] The $S^{141}L$ mutation found in the highly conserved serine 141 resulted in impaired trafficking of TRPM6 to the membrane,[10,18] while the $P^{1017}R$ mutation located in the putative pore-forming region is the only known example of a mutation affecting TRPM6-gating properties without altering assembly or trafficking events.[19] The remaining three-point mutations were found in three Polish families; however, the authors did not report whether HSH was a consequence of either TRPM6 trafficking or functional impairment.[20] Overall, 34 different mutations have been previously described, from which only five are point mutations, thus ~85% of mutations are truncating. This study contributes five previously unknown missense mutations in the *TRPM6* gene leading to HSH. Our patients phenotype showing manifestation in infancy, severe hypomagnesemia at initial presentation with accompanying hypoparathyroidism and hypocalcemia and the mostly subnormal serum Mg^{2+} levels under oral Mg^{2+} supplementation are in accordance with previous publications. Likewise, the dosage of daily oral Mg^{2+} is in the range as that of previously reported[14] (Figure 1).

Solely, patient F46.1 with only one heterozygous missense mutation identified ($E^{872}G$) presented a delayed diagnosis at the age of 4 years, albeit earlier clinical symptoms were found (at 9 months of age). Other patients have been diagnosed after infancy, but these patients mostly had earlier symptoms as well (Schlingmann *et al*[14]). Although it is not possible to draw a definitive conclusion, we believe that episodes of seizures during febrile illness in patient F46.1 could have been initial symptoms of hypomagnesemia.

On the other hand, her initial serum Mg^{2+} levels, the dose of oral Mg^{2+} during maintenance therapy, as well as serum Mg^{2+} levels in the subnormal range achieved with this treatment are not different from patients with truncating mutations, therefore arguing against a milder phenotype.

Electrophysiological analyses showed that all five newly identified TRPM6 mutations result in non-functional ion channels with no major differences in cell surface expression. These data suggest that the mutations do not affect channel expression and trafficking but rather impair channel gating at the plasma membrane. The $L^{708}P$ mutation is located in the N-terminal domain of the TRPM6 protein. Exchange of a leucine with a proline may represent an important remodelling of the N-terminal domain, which can impede proper interaction with other TRPM6 monomers and thereby affect function. The $E^{872}G$ mutation is located in the first intracellular loop, between the first and second transmembrane domain, and may also represent a significant change in channel structure because of missing potential interactions mediated by the glutamic acid bearing its negative charge. The $Y^{1053}C$ mutant is located in the last transmembrane segment. This mutant is, to our knowledge one of the most interesting because of its localization within the sixth transmembrane segment. Mutation of a tyrosine into a cysteine presumably modifies important structural features within the region close to the selectivity filter, leading to impaired function. $L^{1143}P$ is present in the C-terminal domain, close to the highly conserved TRP box. Structural changes in the TRP box structure may affect TRPM6 function, at least for PIP_2, critical for inactivation of the ion channel.[32] The remaining $S^{1754}N$ mutation is located immediately before the kinase domain in the C-terminal domain (Figure 4). Loss of a decisive phosphorylation site close to the α-kinase domain could explain the phenotype observed in the $S^{1754}N$ mutant.

All patients except patient F46.1 display two mutant alleles clearly indicating autosomal-recessive inheritance. In patient F46.1, only one mutant allele (E872G) could be identified together with sequence variant $Q^{1663}R$ of initially unknown significance. This variant is meanwhile listed as a polymorphism in public databases (rs55679040).

As the $Q^{1663}R$ variant was unknown at the time of discovery and parental DNA was not available for analysis, we aimed to investigate the pathophysiological role of mutant $E^{872}G$ and variant $Q^{1663}R$, both detected in patient F46.1.

Extensive functional studies demonstrated that the $Q^{1663}R$ variant exhibits similar channel activity as WT TRPM6. Additionally, there

was no difference observed in EGF-dependent stimulation of TRPM6 channel activity or in divalent block on the inward monovalent currents. Furthermore, co-expression studies of the $E^{872}G$ mutant with either WT TRPM6 or the $Q^{1663}R$ variant were performed. Here, a significant decrease of current density at highly depolarized voltage was seen in both the conditions. This is likely due to impaired function of the tetramer, as cell surface biotinylation demonstrated that plasma membrane expression levels did not change significantly. These data imply that the $E^{872}G$ mutation diminishes the normal function of a WT TRPM6 or $Q^{1663}R$ allele, resulting in lower Na^+ current density amplitude by a significant 50%. These observations are compatible with a typical loss-of-function character of the $E^{872}G$ mutant and argue against a dominant-negative effect of the $E^{872}G$ mutant. Therefore, it appears most likely that our mutation analysis missed the second pathogenic allele in patient F46.1 necessary for the development of recessive disease.

Heterozygous TRPM6$^{+/-}$ mice exhibit mild hypomagnesemia under a normal diet as an indication of a milder phenotype associated with the loss of one *TRPM6* allele.[33,34] Still, the observed difference in serum Mg^{2+} values in these mice is rather low although significant.[33,34] Moreover, the heterozygous deletion of *TRPM6* results in unaffected Mg^{2+} urinary excretion when compared with WT under normal Mg^{2+} diet.[33] In contrast to this situation in mice, measured serum Mg^{2+} values from parents in our study are normal (data not shown), indicating that heterozygous humans are asymptomatic and have no significant change in Mg^{2+} metabolism, not supporting the idea of a milder phenotype in humans. Furthermore, the embryonic lethality observed in homozygous TRPM6 $^{-/-}$ mice also argues for a more severe phenotype in these mice compared with human disease. An increased number of spontaneous abortions has not been described in families of TRPM6 patients. Differences in gene expression or compensatory mechanisms may account for this apparent discrepancy between mice and human phenotypes. Based on these findings, the most likely explanation for the phenotype of the patient remains an undetected second disease-causing allele in patient F46.1.

Taken together, the present study extends the current picture by describing a set of new *TRPM6* missense mutations distributed all over TRPM6 protein. The clinical course confirms previously published data from a larger patient cohort with truncating mutations as well as data published from two patients with point mutations.[14,18] All mutants, display a loss-of-function phenotype. Proper function of TRPM6 appears to be independent from the location of the missense mutation, suggesting that integrity of the whole protein is essential for its proper function. On the other hand, complete loss-of-function of TRPM6 is obviously necessary to provoke the typical HSH phenotype. Therefore, missense mutations showing residual function might account for milder phenotypes yet to be identified.

Interestingly, all mutated amino acids except $L^{1143}P$ are conserved in the closest homolog of TRPM6, TRPM7 as well as among mammals, supporting a proposed role in maintaining structure/function relationships. This could imply, that they represent key elements present in domains within the protein important for membrane assembly and stability of the tetramer. A second option is that these amino acids may determine TRPM6 function by providing docking sites for physiological ligands, signaling proteins, or by interacting with scaffolding proteins that have been shown to be essential for modulating the gating properties of other TRP members.[35]

As hypomagnesemia can be multifactorial and multigenic, studies of isolated monogenic disorders represent a valuable tool to disclose the role of a single gene for Mg^{2+} metabolism. Naturally occurring missense mutations inform about key amino acids involved in the function of such proteins. Additionally, further structure–function studies as well as identification of players involved in TRPM6 modulation will be necessary to better understand how systemic Mg^{2+} regulation takes place and eventually improve current clinical treatments to ameliorate patient's quality of life.

CONFLICT OF INTEREST

The authors declare no conflict of interest.

ACKNOWLEDGEMENTS

We are indebted to the participating patients as well as their families for their kind cooperation in this study. We also thank the following physicians who are taking care of the patients: C Mueller (Remscheid, Germany), L Dupuis (Toronto, Canada), A Zolotnitskaya (Valhalla, NY, USA), J Tolmie (Glasgow, UK), and G Horneff (St Augustin, Germany). Finally, we thank H Dimke for critical discussion. This work was supported by grants of the Hans-Joachim-Bodlee-Foundation and the Netherlands Organization for Scientific Research (NWO-ALW 814.02.001 and ZonMw 9120.8026). JGH is supported by an EURYI award. JVDW is supported by an EMBL-Felowship (ALTF 1535-2010).

1 Smales OR: Primary infantile hypomagnesaemia. *Proc R Soc Med* 1974; **67**: 759–760.
2 Suh SM, Tashjian AH Jr., Matsuo N, Parkinson DK, Fraser D: Pathogenesis of hypocalcemia in primary hypomagnesemia: normal end-organ responsiveness to parathyroid hormone, impaired parathyroid gland function. *J Clin Invest* 1973; **52**: 153–160.
3 Anast CS, Mohs JM, Kaplan SL, Burns TW: Evidence for parathyroid failure in magnesium deficiency. *Science* 1972; **177**: 606–608.
4 Ebel H, Gunther T: Role of magnesium in cardiac disease. *J Clin Chem Clin Biochem* 1983; **21**: 249–265.
5 Packer M: Sudden unexpected death in patients with congestive heart failure: a second frontier. *Circulation* 1985; **72**: 681–685.
6 Milla PJ, Aggett PJ, Wolff OH, Harries JT: Studies in primary hypomagnesaemia: evidence for defective carrier-mediated small intestinal transport of magnesium. *Gut* 1979; **20**: 1028–1033.
7 Matzkin H, Lotan D, Boichis H: Primary hypomagnesemia with a probable double magnesium transport defect. *Nephron* 1989; **52**: 83–86.
8 Quamme GA: Renal magnesium handling: new insights in understanding old problems. *Kidney Int* 1997; **52**: 1180–1195.
9 Dai LJ, Ritchie G, Kerstan D, Kang HS, Cole DE, Quamme GA: Magnesium transport in the renal distal convoluted tubule. *Physiol Rev* 2001; **81**: 51–84.
10 Schlingmann KP, Weber S, Peters M *et al*: Hypomagnesemia with secondary hypocalcemia is caused by mutations in TRPM6, a new member of the TRPM gene family. *Nat Genet* 2002; **31**: 166–170.
11 Walder RY, Landau D, Meyer P *et al*: Mutation of TRPM6 causes familial hypomagnesemia with secondary hypocalcemia. *Nat Genet* 2002; **31**: 171–174.
12 Topala CN, Groenestege WT, Thebault S *et al*: Molecular determinants of permeation through the cation channel TRPM6. *Cell Calcium* 2007; **41**: 513–523.
13 Voets T, Nilius B, Hoefs S *et al*: TRPM6 forms the Mg2+ influx channel involved in intestinal and renal Mg2+ absorption. *J Biol Chem* 2004; **279**: 19–25.
14 Schlingmann KP, Sassen MC, Weber S *et al*: Novel TRPM6 mutations in 21 families with primary hypomagnesemia and secondary hypocalcemia. *J Am Soc Nephrol* 2005; **16**: 3061–3069.
15 Guran T, Akcay T, Bereket A *et al*: Clinical and molecular characterization of Turkish patients with familial hypomagnesaemia: novel mutations in TRPM6 and CLDN16 genes. *Nephrol Dial Transplant* 2012; **27**: 667–673.
16 Habeb AM, Al-Harbi H, Schlingmann KP: Resolving basal ganglia calcification in hereditary hypomagnesemia with secondary hypocalcemia due to a novel TRPM6 gene mutation. *Saudi J Kidney Dis Transpl* 2012; **23**: 1038–1042.
17 Esteban-Oliva D, Pintos-Morell G, Konrad M: Long-term follow-up of a patient with primary hypomagnesaemia and secondary hypocalcaemia due to a novel TRPM6 mutation. *Eur J Pediatr* 2009; **168**: 439–442.
18 Chubanov V, Waldegger S, Mederos y Schnitzler M *et al*: Disruption of TRPM6/TRPM7 complex formation by a mutation in the TRPM6 gene causes hypomagnesemia with secondary hypocalcemia. *Proc Natl Acad Sci USA* 2004; **101**: 2894–2899.
19 Chubanov V, Schlingmann KP, Waring J *et al*: Hypomagnesemia with secondary hypocalcemia due to a missense mutation in the putative pore-forming region of TRPM6. *J Biol Chem* 2007; **282**: 7656–7667.
20 Jalkanen R, Pronicka E, Tyynismaa H, Hanauer A, Walder R, Alitalo T: Genetic background of HSH in three Polish families and a patient with an X;9 translocation. *Eur J Hum Genet* 2006; **14**: 55–62.
21 Ramage IJ, Ray M, Paton RD, Logan RW, Beattie TJ: Hypomagnesaemic tetany. *J Clin Pathol* 1996; **49**: 343–344.

22 al-Ghamdi SM, Cameron EC, Sutton RA: Magnesium deficiency: pathophysiologic and clinical overview. *Am J Kidney Dis* 1994; **24**: 737–752.
23 Trouet D, Nilius B, Voets T, Droogmans G, Eggermont J: Use of a bicistronic GFP-expression vector to characterise ion channels after transfection in mammalian cells. *Pflugers Arch* 1997; **434**: 632–638.
24 Stuiver M, Lainez S, Will C *et al*: CNNM2, encoding a basolateral protein required for renal Mg2+ handling, is mutated in dominant hypomagnesemia. *Am J Hum Genet* 2011; **88**: 333–343.
25 de Groot T, van der Hagen EA, Verkaart S, te Boekhorst VA, Bindels RJ, Hoenderop JG: Role of the transient receptor potential vanilloid 5 (TRPV5) protein N terminus in channel activity, tetramerization, and trafficking. *J Biol Chem* 2011; **286**: 32132–32139.
26 Runnels LW, Yue L, Clapham DE: TRP-PLIK, a bifunctional protein with kinase and ion channel activities. *Science* 2001; **291**: 1043–1047.
27 Nadler MJ, Hermosura MC, Inabe K *et al*: LTRPC7 is a Mg.ATP-regulated divalent cation channel required for cell viability. *Nature* 2001; **411**: 590–595.
28 Li M, Du J, Jiang J *et al*: Molecular determinants of Mg2+ and Ca2+ permeability and pH sensitivity in TRPM6 and TRPM7. *J Biol Chem* 2007; **282**: 25817–25830.
29 Groenestege WM, Thebault S, van der Wijst J *et al*: Impaired basolateral sorting of pro-EGF causes isolated recessive renal hypomagnesemia. *J Clin Invest* 2007; **117**: 2260–2267.
30 San-Cristobal P, Dimke H, Hoenderop JG, Bindels RJ: Novel molecular pathways in renal Mg2+ transport: a guided tour along the nephron. *Curr Opin Nephrol Hypertens* 2010; **19**: 456–462.
31 Apa H, Kayserili E, Agin H, Hizarcioglu M, Gulez P, Berdeli A: A case of hypomagnesemia with secondary hypocalcemia caused by Trpm6 gene mutation. *Indian J Pediatr* 2008; **75**: 632–634.
32 Xie J, Sun B, Du J *et al*: Phosphatidylinositol 4,5-bisphosphate (PIP(2)) controls magnesium gatekeeper TRPM6 activity. *Sci Rep* 2011; **1**: 146.
33 Woudenberg-Vrenken TE, Sukinta A, van der Kemp AW, Bindels RJ, Hoenderop JG: Transient receptor potential melastatin 6 knockout mice are lethal whereas heterozygous deletion results in mild hypomagnesemia. *Nephron Physiol* 2011; **117**: p11–p19.
34 Walder RY, Yang B, Stokes JB *et al*: Mice defective in Trpm6 show embryonic mortality and neural tube defects. *Hum Mol Genet* 2009; **18**: 4367–4375.
35 Zhang X, Li L, McNaughton PA: Proinflammatory mediators modulate the heat-activated ion channel TRPV1 via the scaffolding protein AKAP79/150. *Neuron* 2008; **59**: 450–461.